25. Boson B, Granio O, Bartenschlager R, Cosset F (2011) A concerted action of hepatitis C virus p7 and nonstructural protein 2 regulates core localization at the endoplasmic reticulum and virus assembly. PLoS Pathog. 7: e1002144.
26. Gentzsch J, Brohm C, Steinmann E, Friesland M, Menzel N, et al. (2013) Hepatitis C virus p7 is critical for capsid assembly and envelopment. PLoS Pathog. 9: e1003355.
27. Shavinskaya A, Boulant S, Penin F, McLauchlan J, Bartenschlager R. (2007) The lipid droplet binding domain of hepatitis C virus core protein is a major determinant for efficient virus assembly. J. Biol. Chem. 282: 37158-37169.
28. Ai L, Lee Y, Chen SS (2009) Characterization of hepatitis C virus core protein multimerization and membrane envelopment: revelation of a cascade of core-membrane interactions. J. Virol. 83: 9923-9939.
29. Mei X, Atkinson D (2011) Crystal structure of C-terminal truncated apolipoprotein A-1 reveals the assembly of high density lipoprotein (HDL) by dimerization. J. Biol. Chem. 286: 38570-38582.
30. Rozek A, Sparrow JT, Weisgraber KH, Cushley JR (1999) Conformation of human apolipoprotein C-1 in a lipid-mimetic environment determined by CD and NMR spectrometry. Biochemistry. 38: 14475-14484.
31. Eichinger A, Nasreen A, Jin H (2007) Structural insight into the dual ligand specificity and mode of high density lipoprotein association of apolipoprotein D. J. Biol. Chem. 282: 31068-31075.
32. Chen J, Li Q, Wang J (2011) Topology of human apolipoprotein E3 uniquely regulates its diverse biological functions. Proc. Natl. Acad. Sci. U. S. A. 108: 14813-14818.
33. Schwarzenbacher R, Zeth K, Diederichs K, Gries A, Kostner GM, et al. (1999) Crystal structure of human β2-glycoprotein 1: implication for phospholipid binding and the antiphospholipid syndrome. EMBO J. 18: 6228-6239.
34. Sevvana M, Kassler K, Ahnstrom J, Weiler S, Dahlback B, et al. (2010) Mouse ApoM displays an unprecedented seven-stranded lipocalin fold: folding decoy or alternative native fold? J. Mol. Biol. 404: 363-371.
35. Nielsen SU, Bassendine MF, Burt AD, Martin C, Pumeechockchai W, et al. (2006) Association between hepatitis C virus and very-low-density lipoprotein (VLDL)/LDL analyzed in iodixanol density gradients. J. Virol. 80: 2418-2428.
36. Jammart B, Michelet M, Pecheur E, Parent R, Bartosch B, et al. (2013) Very-low-density lipoprotein (VLDL)-prpducing and hepatitis C virus-replicating HepG2 cells secrete no more lipoviroparticles than VLDL-deficient Huh7.5 cells. J. Virol. 87: 1405-1412.
37. Hueging K, Doepke M, Vieyres G, Bankwitz D, Frentzen A, et al. (2014) Apolipoprotein E codetermines tissue tropism of hepatitis C virus and is crucial for viral cell-to-cell transmission by contributing to a postenvelopment step of assembly. J. Virol. 88: 1433-1466.
38. Coller KE, Heaton NS, Berger KL, Cooper JD, Saunders JL, et al. (2012) Molecular determinants and dynamics of hepatitis C virus secretion. PLoS Pathog. 8: e1002466.
39. Catanese TM, Uryu K, Kopp M, Edwards TJ, Andrus L, et al. (2013) Ultrastructural analysis of hepatitis C virus particles. Proc. Natl. Acad. Sci. U. S. A. 110: 9505-9510.
40. Cheng G, Montero A, Gastaminza P, Whitten-Bauer C, Wieland SF, et al. (2008) A virocidal amphipathic α-helical peptide that inhibits hepatitis C virus infection *in vitro*. Proc. Natl. Acad. Sci. U. S. A. 105: 3088-3093.
41. Scarselli E, Ansuini H, Cerino R, Roccasecca RM, Acali S, et al. (2002) The human scavenger receptor class B type 1 is a novel candidate receptor for the hepatitis C virus. EMBO J. 21: 5017-5025.
42. Molina S, Castet V, Fournier-Wirth C, Pichard-Garcia L, Avner R, et al. (2007) The low-density lipoprotein receptor plays a role in the infection of primary human hepatocytes by hepatitis C virus. J. Hepatol. 46: 411-419.

43. Owen DM, Huang H, Ye J, Gale MJ (2009) Apolipoprotein E on hepatitis C virion facilitates infection through interaction with low-density lipoprotein receptor. Virology. 394: 99-108.
44. Prentoe J, Serre SB, Ramirez S, Nicosia A, Gottwein JM, et al. (2014) Hypervariable region 1 deletion and required adaptive envelope mutations confer decreased dependency on scavenger receptor class B type 1 and low density lipoprotein receptor for hepatitis C virus. J. Virol. 88: 1725-1739.
45. Meunier J, Russell RS, Engle RE, Faulk KN, Purcell RH, et al. (2008) Apolipoprotein C1 association with hepatitis C virus. J. Virol. 82: 9647-9656.
46. Dreux M, Boson B, Ricard-Blum S, Molle J, Lavillette D et al. (2007) The exchangeable apolipoprotein ApoC-1 promotes membrane fusion of hepatitis C virus. J. Biol. Chem. 282: 32357-32369.
47. Fukuhara T, Matsuura Y (2013) Role of miR-122 and lipid metabolism in HCV infection. J. Gastroenterol. 48: 169-176.
48. Ploss A, Evans MJ, Gaysinskaya VA, Panis M, You H, et al. (2009) Human occludin is a hepatitis C virus entry factor required for infection of mouse cells. Nature. 457: 882-886.
49. Mercer DF, Schiller DE, Elliott JF, Douglas DN, Hao C, et al. (2001) Hepatitis C virus replication in mice with chimeric human livers. Nat. Med. 7: 927-933.
50. Dorner M, Horwitz JA, Donovan BM, Labitt RN, Budell BC, et al. (2013) Completion of the entire hepatitis C virus life cycle in genetically humanized mice. Nature. 501: 237-241.
51. Wang H, Yang H, Shivalila CS, Dawlaty MM, Cheng AW, et al. (2013) One-step generation of mice carrying mutations in multiple genes by CRISPR/Cas-mediated genome engineering. Cell. 153: 910-918.
52. Cho SW, Kim S, Kim JM, Kim J (2013) Targeted genome engineering in human cells with the Cas9 RNA-guided endonuclease. Nat. Biotechnol. 31: 230-232.
53. Shalem O, Sanjana NE, Hartenian E, Shi X, Scott DA, et al. (2014) Genome-scale CRISPR-Cas9 knockout screening in human cells. Science. 343: 84-87.
54. Fukuhara T, Kambara H, Shiokawa M, Ono C, Katoh H, et al. (2012) Expression of microRNA miR-122 facilitates an efficient replication in nonhepatic cells upon infection with hepatitis C virus. J. Virol. 86: 7918-7933.
55. Russell RS, Meunier JC, Takikawa S, Faulk K, Engle RE, et al. Advantages of a single-cycle production assay to study cell culture-adaptive mutations of hepatitis C virus. Proc. Natl. Acad. Sci. U. S. A. 105: 4370-4375 (2008).
56. Guschin YD, Waite AJ, Katibah GE, Miller JC, Holmes MC, et al. (2010) A rapid and general assay for monitoring endogenous gene modification. Methods Mol. Biol. 649: 247-256 (2010).
57. Rieder CL, Bowser SS (1985). Correlative immunofluorescence and electron microscopy on the same section of epon-embedded material. J. Histochem. Cytochem. 33: 165-171.

Figure Legends

Figure 1. Several apolipoproteins participate in HCV propagation. (A) Relative mRNA expression of the apolipoproteins in the liver tissues (left columns) was determined using the NextBio Body Atlas application. The median expression (right columns) was calculated across all 128 human tissues from 1,068 arrays using the Affymetrix GeneChip© Human Genome U133 Plus 2.0 Array. mRNA expression for each gene was log10 transformed. (B) Log10 transformed, normalized signal intensity of the apolipoproteins in Huh7 (left columns) and HepG2 (right columns) cells were extracted from previously published expression microarray dataset GSE32886. (C) Huh7 cells infected with HCVcc at an MOI of 1 at 6 h post-transfection with siRNAs targeting ApoA2 (A2), ApoB (B), ApoE (E) and control (Cont), and expression levels of apolipoproteins (upper panel) and infectious titers in the culture supernatants (lower panel) were determined by immunoblotting and a focus-forming assay at 72 h post-infection, respectively. (D) ApoA1, ApoA2, ApoC1, ApoE and ApoH were exogenously expressed in control and ApoE-knockdown Huh7 cells

by lentiviral vectors. Expressions of the apolipoproteins were determined by immunoblotting analysis. (E) Infectious titers in the culture supernatants of control and ApoE-knockdown Huh7 cells expressing the apolipoproteins were determined by focus-forming assay at 72 h post-infection. In all cases, asterisks indicate significant differences (*, $P < 0.05$; **, $P < 0.01$) versus the results for control cells.

Figure 2. ApoB and ApoE redundantly participate in the formation of infectious HCV particles. (A) Huh7 and E-KO1 cells were infected with HCVcc at an MOI of 1 at 6 h post-transfection with siRNAs targeting ApoB or ApoE, and infectious titers in the culture supernatants were determined by focus-forming assay at 72 h post-infection. (B) HCVpp were inoculated into Huh7, BE-KO1 and BE-KO2 cells, and luciferase activities were determined at 48 h post-infection. (C) A subgenomic HCV RNA replicon of the JFH1 strain was electroporated into BE-KO1 and BE-KO2 cells with/without expression of ApoE by lentiviral vector (ApoE-res), and the colonies were stained with crystal violet at 31 days post-electroporation after selection with 400 μg/ml of G418. Huh7, BE-KO1 and BE-KO2 cells were infected with HCVcc at an MOI of 1, and intracellular HCV RNA (D) and infectious titers in the supernatants (E) were determined at 72 h post-infection by qRT-PCR and focus-forming assay, respectively. (F) Exogenous expression of ApoE in BE-KO1 and BE-KO2 cells by lentiviral vector was determined by immunoblotting analysis. (G) Infectious titers in the culture supernatants of BE-KO1 (gray bars) and ApoE-res cells (red bars) infected with HCVcc at an MOI of 1 were determined at 72 h post-infection by focus-forming assay.

Figure 3. MTTP participates in the formation of infectious HCV particles through the maturation of ApoB. (A) Expressions of ApoB, ApoE and MTTP in Huh7, B-KO1, M-KO1, E-KO1, BE-KO1 and EM-KO1 cells were determined by immunoblotting analysis. Cells were infected with HCVcc at an MOI of 1, and intracellular HCV RNA (B) and infectious titers in the supernatants (C) were determined at 72 h post-infection by qRT-PCR and focus-forming assay, respectively. The expressions of ApoB, ApoE and MTTP in BE-KO1 and EM-KO1 cells with/without expression of ApoE or MTTP by lentiviral vector were determined by immunoblotting (D) and ELISA (E). Cells were infected with HCVcc at an MOI of 1, and intracellular HCV RNA (F) and infectious titers in the supernatants (G) were determined at 72 h post-infection by qRT-PCR and focus-forming assay, respectively.

Figure 4. Exchangeable apolipoproteins redundantly participate in the formation of infectious HCV particles. (A) BE-KO1 cells infected with HCVcc at an MOI of 1 at 6 h post-transfection with siRNAs targeting ApoA1 (A1), ApoA2 (A2), ApoC1 (C1), ApoC2 (C2), ApoC3 (C3) and ApoH (H) and infectious titers in the culture supernatants were determined by focus-forming assay at 72 h post-infection. (B) ApoA1, ApoA2, ApoC1, ApoC2, ApoC3, ApoE and ApoH were exogenously expressed in BE-KO1 cells by infection with lentiviral vectors, and then infected with HCVcc at an MOI of 1. Expression of the apolipoproteins was determined by immunoblot analysis (upper), and infectious titers in the culture supernatants were determined at 72 h post-infection by focus-forming assay (lower). (C) Extracellular and intracellular HCV RNA in BE-KO1 cells expressing apolipoproteins and infected with HCVcc were determined at 72 h post-infection by qRT-PCR. (D) Specific infectivity was calculated as extracellular infectious titers / extracellular HCV RNA copies in BE-KO1 cells expressing apolipoproteins at 72 h post-infection. (E) 293T cells stably expressing CLDN1 and miR-122 (293T-CLDN/miR-122 cells) were infected with the lentiviral vectors, and the expressions of the apolipoproteins were determined by immunoblot analysis (upper). These cells were infected with HCVcc at an MOI of 1, and infectious titers in the supernatants were determined at 72 h post-infection by focus-forming assay (lower). In all cases, asterisks indicate significant differences (*, $P < 0.05$; **, $P < 0.01$) versus the results for control cells.

Figure 5. Exchangeable apolipoproteins participate in the formation of infectious HCV particles of genotype 1 and 3. ApoA1, ApoA2, ApoC1, ApoC2, ApoC3, ApoE and ApoH were exogenously expressed in BE-KO1 cells by infection with lentiviral vectors, and then infected with

genotype 1b and 3a chimeric HCVcc, TH/JFH1 (A) and S310/JFH1 (B) at an MOI of 0.5. Intracellular HCV RNA and infectious titers in the culture supernatants were determined at 72 h post-infection by qRT-PCR (upper) and focus-forming assay (lower). Asterisks indicate significant differences (**, $P < 0.01$) versus the results for control cells.

Figure 6. Accumulation of core proteins around lipid droplets in BE-KO1 cells. (A) Extracellular and intracellular infectious titers in Huh7, BE-KO1 and ApoE-restored cells infected by lentiviral vector (ApoE-res) were determined at 72 h post-infection with HCVcc at an MOI of 1 by focus-forming assay. Asterisks indicate significant differences (**, $P < 0.01$) versus the results for parental cells. (B) BE-KO1 cells infected with HCVcc at an MOI of 1 were stained with anti-Core antibody at 72 h post-infection and examined by fluorescence microscopy. Identical fields were observed under electron microscopy by using the correlative FM-EM technique. The boxed areas are magnified and displayed. Huh7, BE-KO1 and ApoE-res cells infected with HCVcc at an MOI of 1 were subjected to immunofluorescence analyses by using anti-Core antibody (C), and immunoblotting by using antibodies against Core, NS3, ApoE, and actin at 72 h post-infection (D). Lipid droplets and cell nuclei were stained by BODIPY and DAPI, respectively. (E) BE-KO1 and ApoE-res cells infected with Jc1 strain-based HCVcc (HCVcc/Jc1; left panel) or JFH1 strain-based HCVcc (HCVcc/JFH1; right panel) at an MOI of 1 were subjected to immunofluorescence analysis by using anti-Core antibody at 72 h post-infection. Lipid droplets and cell nuclei were stained by BODIPY and DAPI, respectively.

Figure 7. Apolipoproteins participate in the post-envelopment step of the HCV life cycle. The supernatants (A) and lysates (B) of BE-KO1 and ApoE-restored (ApoE-res) cells infected with HCVcc at an MOI of 1 were subjected to density gradient fractionation. Each fraction was subjected to immunoblotting using anti-Core antibody (upper). The infectious titers and densities of each fraction were determined (lower). (C) The lysates of BE-KO1 and ApoE-res cells infected with HCVcc at an MOI of 1 were subjected to proteinase K digestion protection assay. Lysates were separated into 3 parts and incubated for 1 h on ice in the presence or absence of 50 μg/ml proteinase K with/without pretreatment with 5% Triton-X and then subjected to immunoblotting.

Figure 8. Amphipathic α-helices in apolipoproteins participate in the infectious particle formation of HCV. (A) Predicted or experimentally determined secondary structures of apolipoproteins. Secondary structures of the helices and sheets in the apolipoproteins are colored red and cyan, respectively. The three-dimensional structures of ApoA1 (Protein Data Bank (PDB) ID, 3R2P), ApoC1 (PDB ID, 1IOJ), ApoD (PDB ID, 2HZR), ApoE (PDB ID, 2L7B), ApoH (PDB ID, 1C1Z) and ApoM (PDB ID, 2XKL) are also shown in a ribbon model using the same color code of secondary structures. In cases in which the structure was not available, the secondary structure was predicted by using a CLC Genomics Workbench. (B,C) Schematics of the ApoE- and ApoC1-deletion mutants (upper). Deletion mutants with HA tags expressed in BE-KO1 cells by lentiviral vectors were detected by immunoblotting (middle). BE-KO1 cells expressing the WT or deletion mutants of ApoE or ApoC1 were infected with HCVcc at an MOI of 1, and infectious titers in the culture supernatants were determined by focus-forming assay at 72 h post-infection. Asterisks indicate significant differences (**, $P < 0.01$) versus the results for control cells. (D) Schematic of the concentration of viral particles from HCV-infected cells using ultracentrifugation. (E) BE-KO1 cells expressing the WT or deletion mutants of ApoE were infected with HCVcc at an MOI of 1. Culture supernatants harvested at 72 h post-infection were concentrated by ultracentrifugation at 32,000 rpm for 2 h at 4 °C, and subjected to immunoblotting.

Supporting Information

Supporting Figure Legends

Figure S1. Establishment of ApoB- or ApoE-knockout Huh7 cell lines. Target sequences of ZFNs to ApoB (A) and ApoE (B) are indicated by red characters inside a red box at the top of the panel. Gene knockout by the sequence modification in the 2 alleles of the ApoB (A) or ApoE (B)

763 gene in knockout cell lines (B-KO1 and B-KO2, or E-KO1 and E-KO2) is shown. Deletion and
764 insertion of the sequences are indicated by dotted lines and blue characters in brackets, respectively.
765 Absence of the expressions of ApoB (C) and ApoE (D) in the knockout cell lines was confirmed by
766 immunoblotting using anti-ApoB and -ApoE antibodies. Expression of ApoB (E) and ApoE (F) in
767 the culture supernatants of 293T, Huh7 and the knockout cell lines was determined by ELISA.
768 **Figure S2. Both ApoB and ApoE are involved in the formation of infectious HCV particles.**
769 (A) HCVpp were inoculated into Huh7, B-KO1, B-KO2, E-KO1 and E-KO2 cells, and luciferase
770 activities were determined at 48 h post-infection. (B) A subgenomic HCV RNA replicon of the JFH1
771 strain was electroporated into Huh7, B-KO1 and E-KO1 cells, and colonies were stained with crystal
772 violet at 31 days post-electroporation after selection with 400 μg/ml of G418. HCVcc were
773 inoculated into Huh7, B-KO1, B-KO2, E-KO1 and E-KO2 cells at an MOI of 1 and intracellular
774 HCV RNA at 12, 24, 36 and 60 h post-infection (C), and infectious titers in the culture supernatants
775 at 72 h post-infection (D) were determined by qRT-PCR and focus-forming assay, respectively. (E)
776 Exogenous expression of ApoE in E-KO1 and E-KO2 cells by lentiviral vector was determined by
777 immunoblotting analysis (upper), and infectious titers in the culture supernatants of cells infected
778 with HCVcc at an MOI of 1 were determined at 72 h post-infection by focus-forming assay (lower).
779 **Figure S3. Establishment of ApoB and ApoE double-knockout (BE-KO) Huh7 cell lines.** Gene
780 knockout by the ZFN in the 2 alleles of the ApoB and ApoE genes in the double-knockout cell lines,
781 BE-KO1 (A) and BE-KO2 (B), is shown. Deletion and insertion of the sequences are indicated by
782 dotted lines and blue characters in brackets, respectively. (C) The absence of the expressions of
783 ApoB and ApoE in BE-KO1 and BE-KO2 was confirmed by immunoblotting using anti-ApoB and
784 -ApoE antibodies. Expression of ApoB (D) and ApoE (E) in the culture supernatants of 293T, Huh7,
785 BE-KO1 and BE-KO2 cells was determined by ELISA.
786 **Figure S4. Establishment of MTTP-knockout (M-KO) and ApoE and MTTP**
787 **double-knockout (EM-KO) Huh7 cell lines.** (A) Gene knockout by the ZFN in the 2 alleles of the
788 MTTP gene in the knockout cell lines, M-KO1 and M-KO2, is shown. (B) Expression of MTTP in
789 Huh7, M-KO1 and M-KO2 cells was determined by immunoblotting. Expression of ApoB (C) and
790 ApoE (D) in the culture supernatants of Huh7, M-KO1, M-KO2 and 293T cells was determined by
791 ELISA. (E) Gene knockout in the 2 alleles of the MTTP genes by the CRISPR/Cas9 system and in
792 one allele of the ApoE gene by the ZFN in the double-knockout cell lines, EM-KO1 and EM-KO2,
793 is shown. (F) Expression of MTTP in Huh7, EM-KO1 and EM-KO2 cells was determined by
794 immunoblotting. Expression of ApoB (G) and ApoE (H) in the culture supernatants of Huh7,
795 EM-KO1, EM-KO2 and 293T cells was determined by ELISA. (I) Expression of ApoB mRNA in
796 Huh7, M-KO1, M-KO2, EM-KO1, EM-KO2 and 293T cells was determined by qRT-PCR.
797 **Figure S5. Gene silencing of apolipoproteins.** BE-KO1 cells infected with HCVcc at an MOI of 1
798 at 6 h post-transfection with siRNAs targeting ApoA1, ApoA2, ApoC1, ApoC2, ApoC3 and ApoH,
799 and the expression levels of these apolipoproteins were determined by q-RT PCR using specific
800 primers and probes.
801 **Figure S6. ApoD, ApoL1, and ApoO do not participate in the formation of infectious HCV**
802 **particles.** Exogenous expression of ApoD, ApoE, ApoL1 and ApoO in BE-KO1 cells by lentiviral
803 vector was determined by immunoblotting analysis (upper), and infectious titers in the culture
804 supernatants of cells infected with HCVcc at an MOI of 1 were determined at 72 h post-infection by
805 focus-forming assay (lower).
806 **Figure S7. BE-KO1 cells permit propagation of JEV and DENV.** Huh7, BE-KO1 and
807 ApoE-restored (ApoE-res) cells were infected with JEV and DENV at an MOI of 0.1, and infectious
808 titers in the culture supernatants were determined by focus-forming assay at 48 h post-infection.
809 **Figure S8. Figure S8. Localization of core, NS5A proteins and ER in BE-KO Huh7 cells.**
810 BE-KO1 cells infected with HCVcc at an MOI of 1 were subjected to immunofluorescence analyses
811 by using antibodies against core, NS5A and Calnexin.

Fukuhara et al. Fig. 1

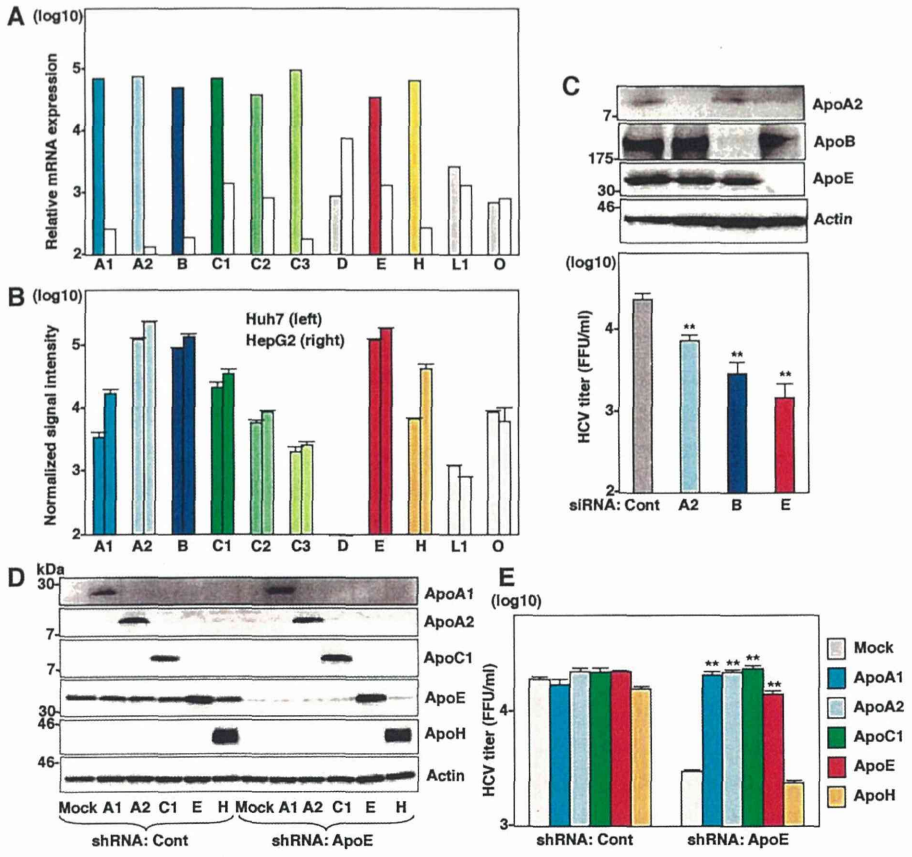

Fukuhara et al. Fig. 2

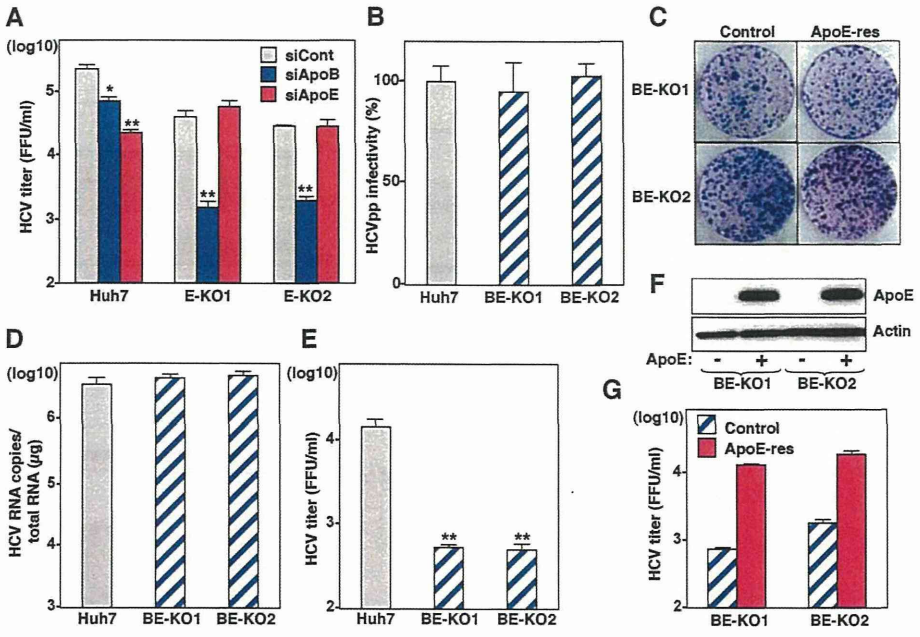

Fukuhara et al. Fig. 3

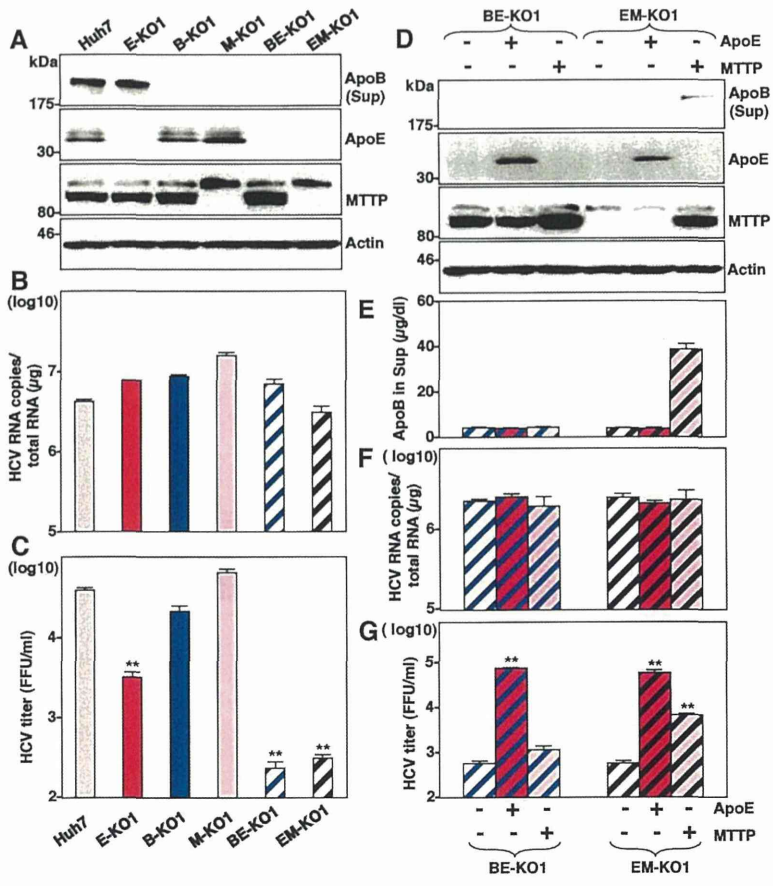

Fukuhara et al. Fig. 4

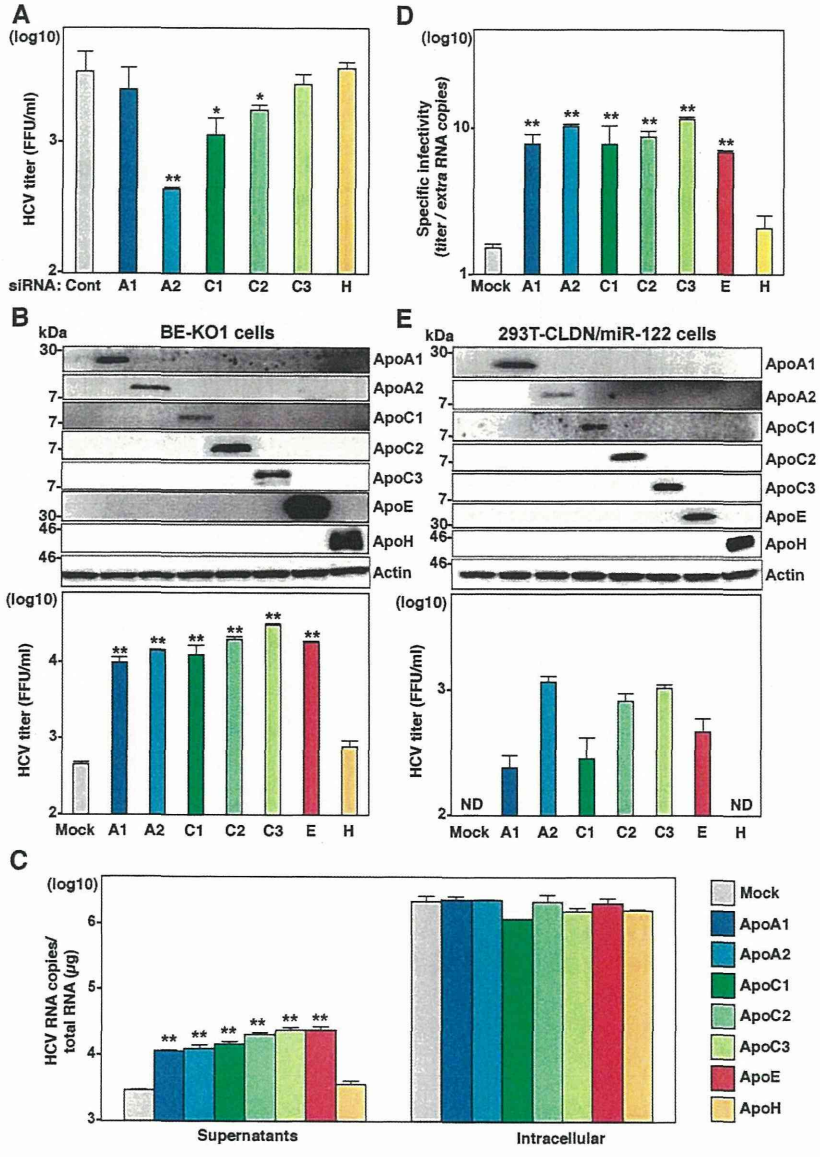

Fukuhara et al. Fig. 5

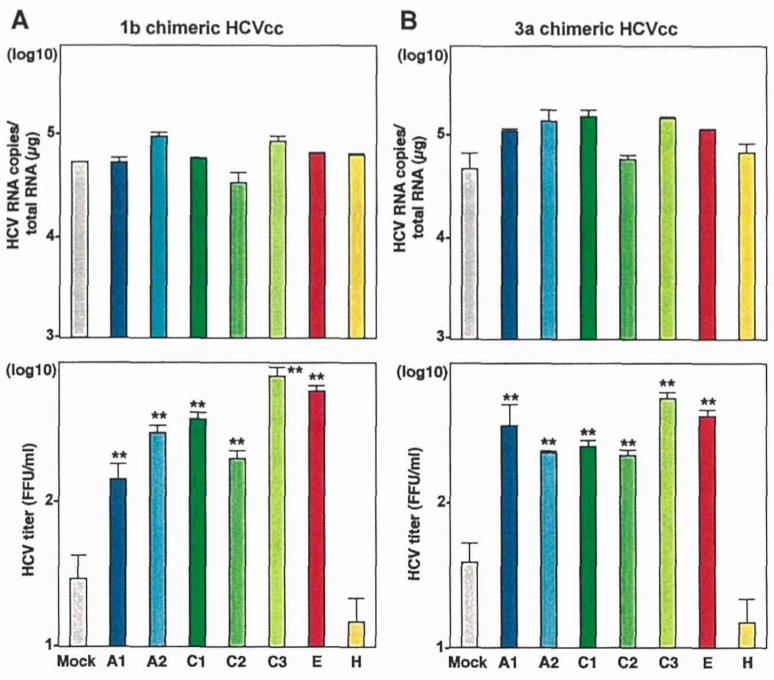

Fukuhara et al. Fig. 6

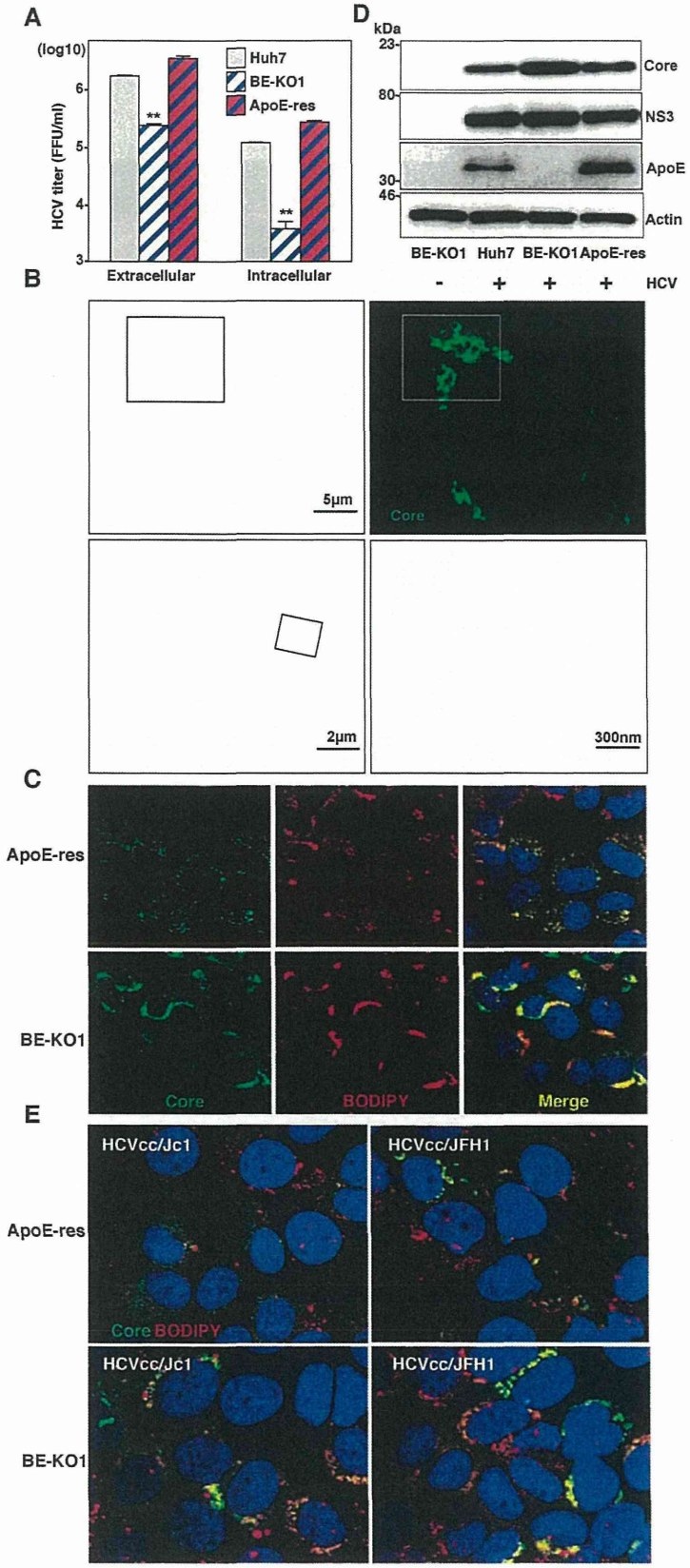

Fukuhara et al. Fig. 7

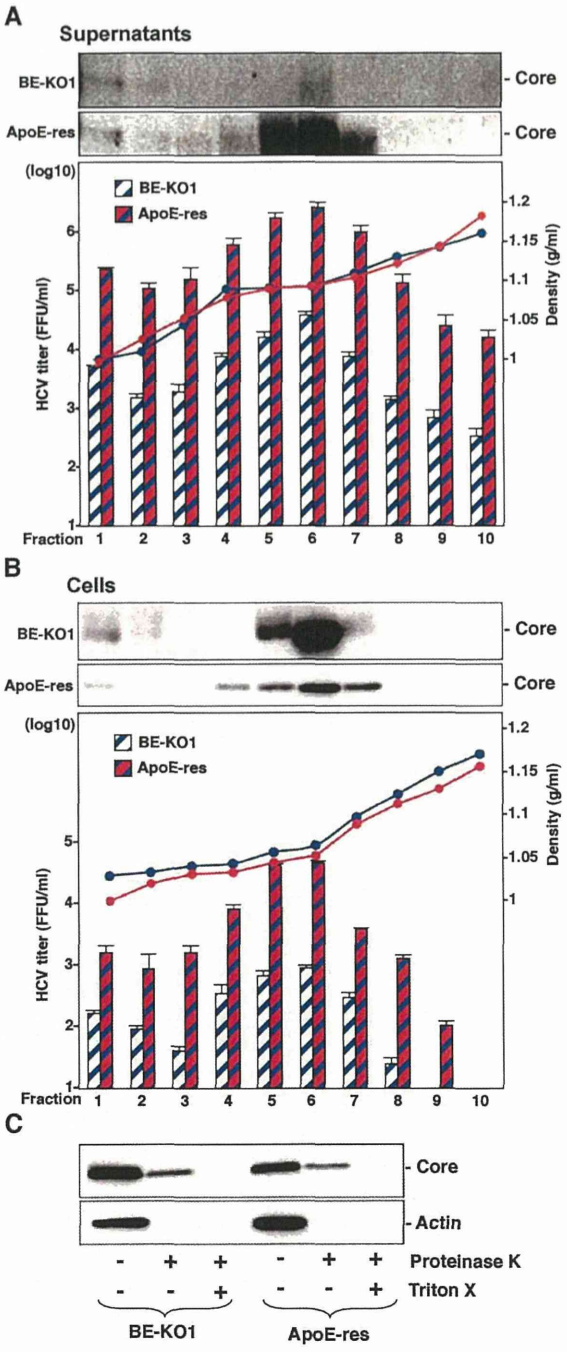

Fukuhara et al. Fig. 8

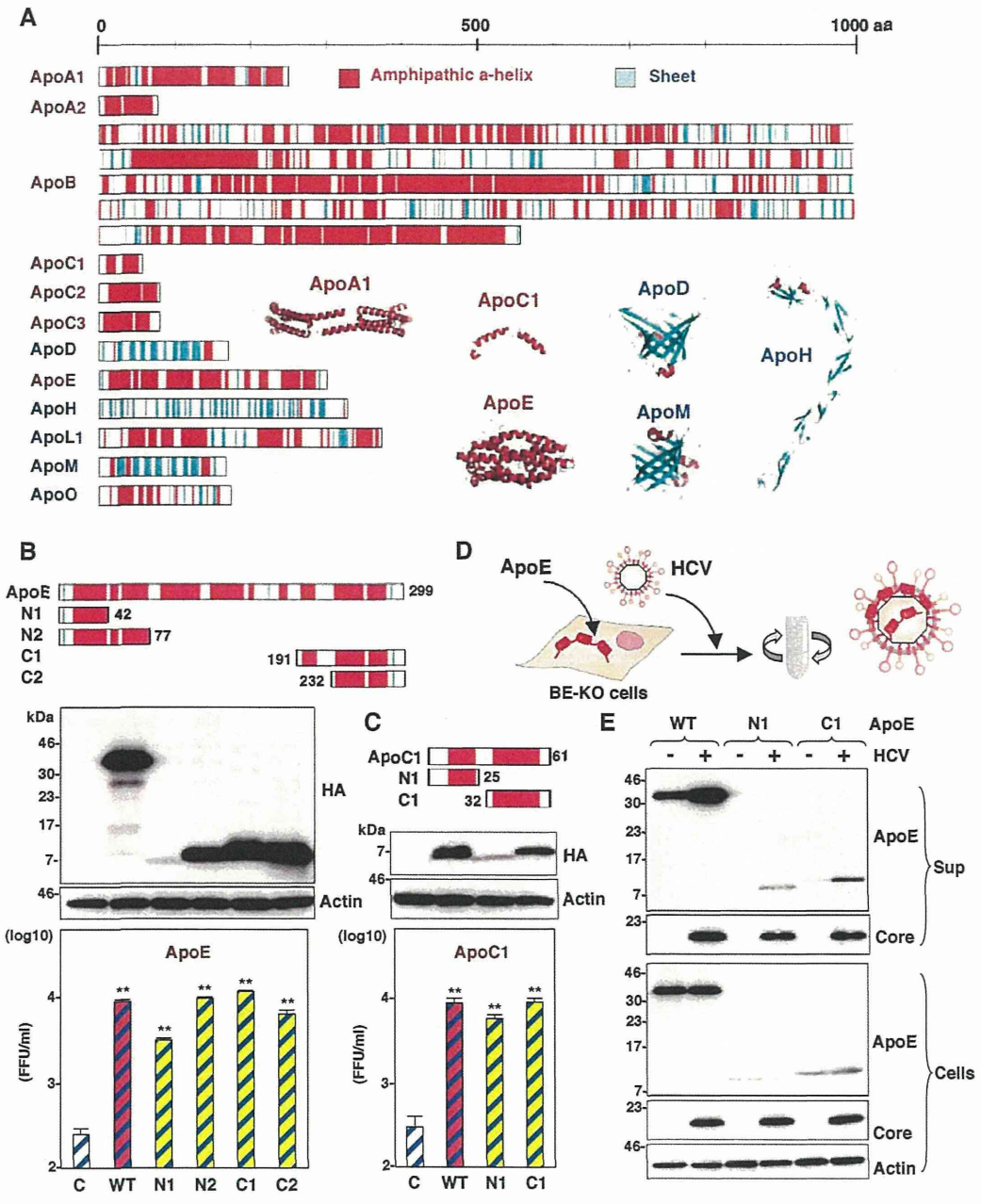

Fukuhara et al. Supplemental Fig. 1

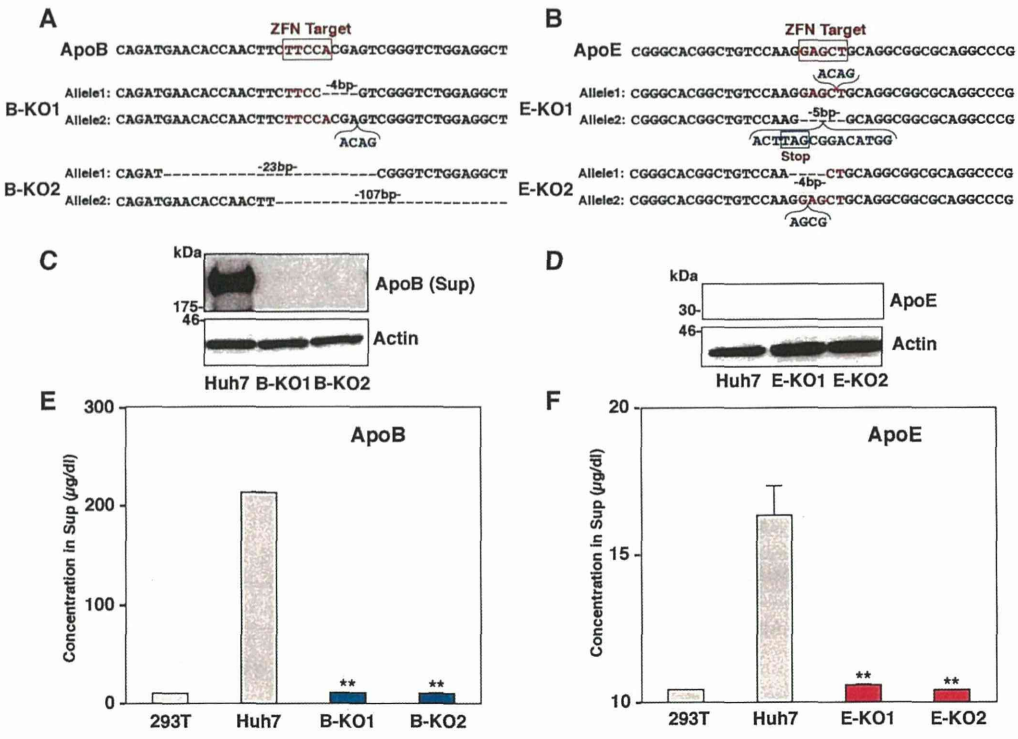

Fukuhara et al. Supplemental Fig. 2

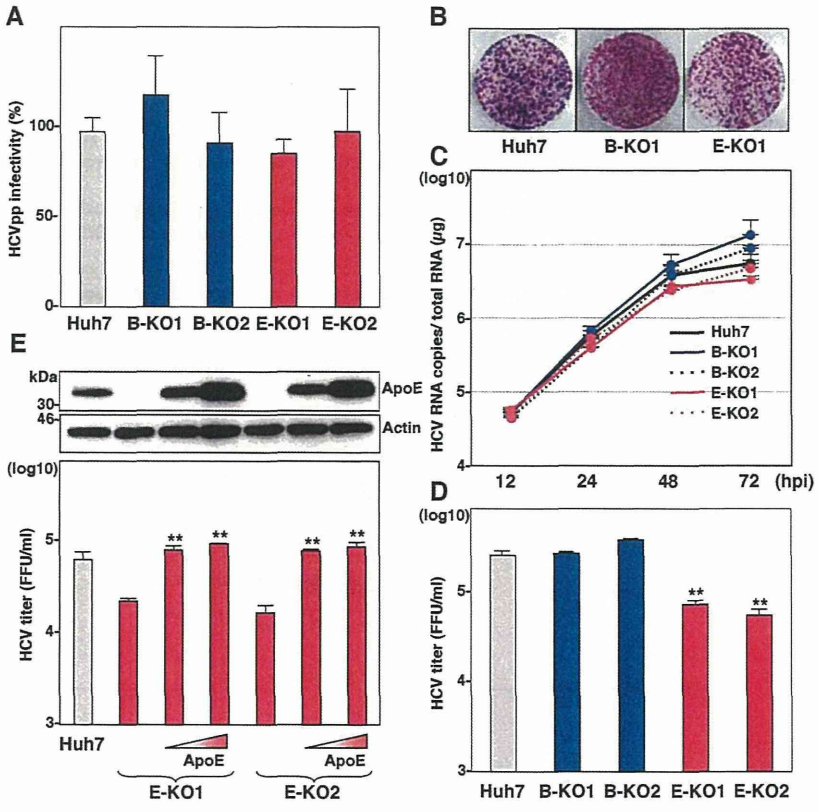

Fukuhara et al. Supplemental Fig. 3

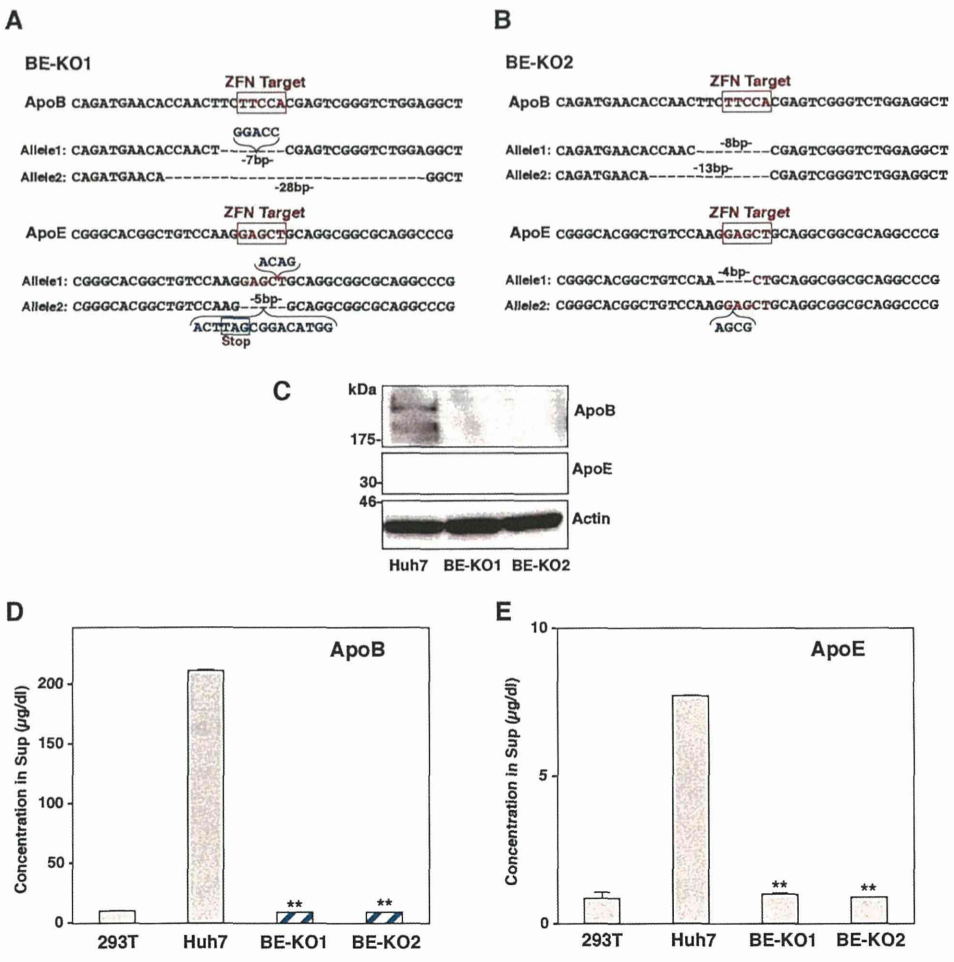

Fukuhara et al. Supplemental Fig. 4

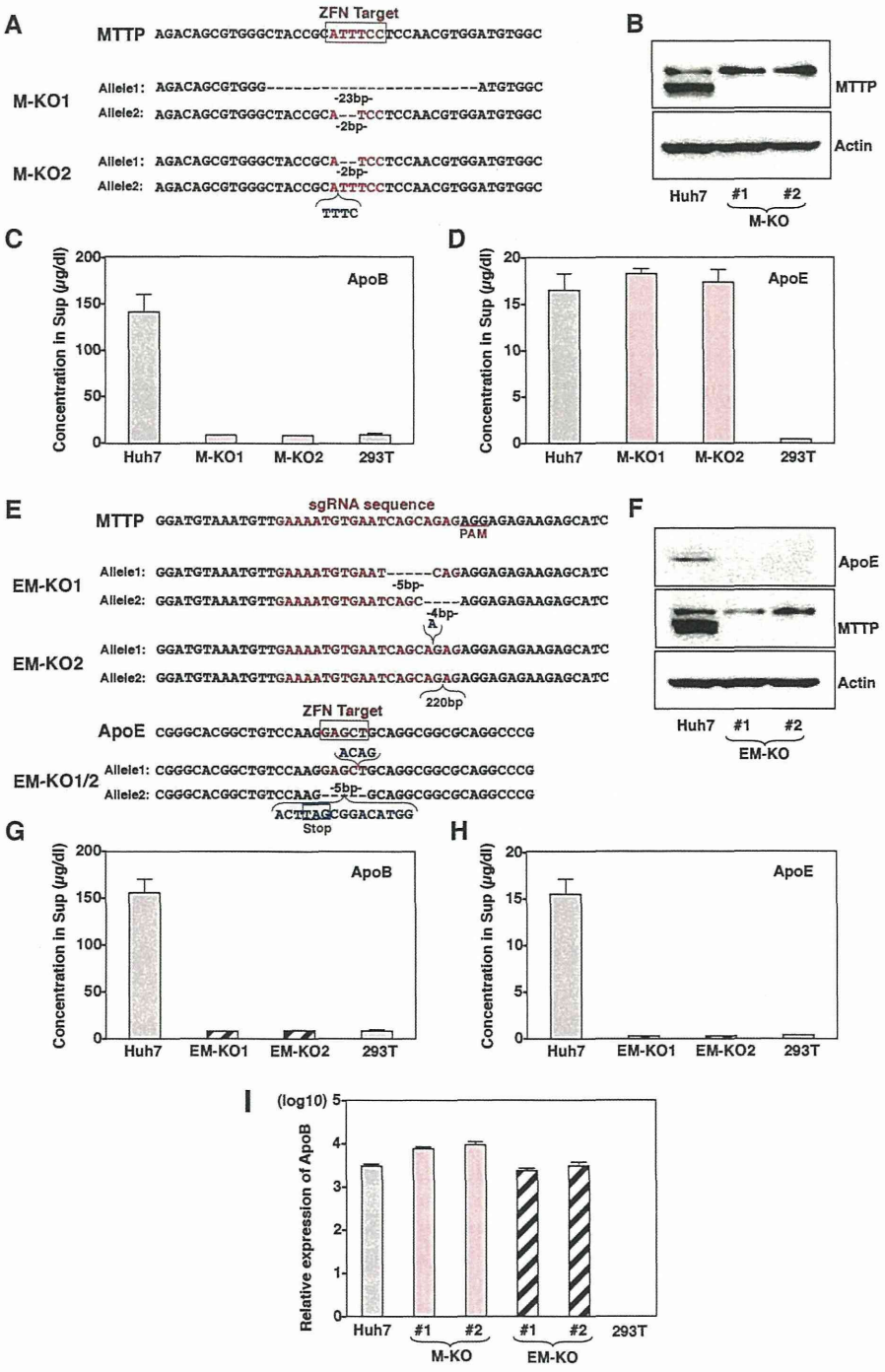

Fukuhara et al. Supplemental Fig. 5

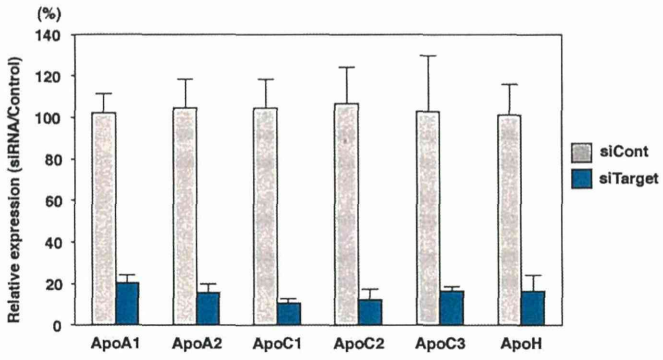

Fukuhara et al. Supplemental Fig. 6

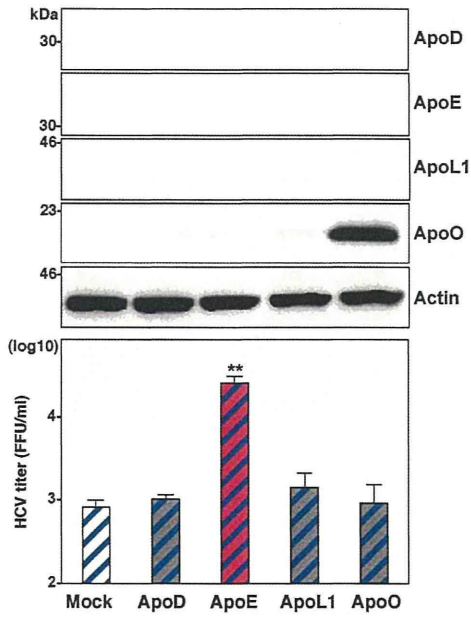

Fukuhara et al. Supplemental Fig. 7